

Glycomic Analysis of Membrane Glycoproteins with Bisecting Glycosylation from Ovarian Cancer Tissues Reveals Novel Structures and Functions

Heba Allam,^{||} Kazuhiro Aoki,[†] Benedict B. Benigno,[§] John F. McDonald,^{‡,§} Samuel G. Mackintosh,^{||} Michael Tiemeyer,[†] and Karen L. Abbott^{*,||}

[†]Complex Carbohydrate Research Center and Department of Biochemistry and Molecular Biology, University of Georgia, 315 Riverbend Road, Athens, Georgia 30602, United States

[‡]School of Biology, Georgia Institute of Technology, 310 Ferst Drive, Atlanta, Georgia 30332, United States

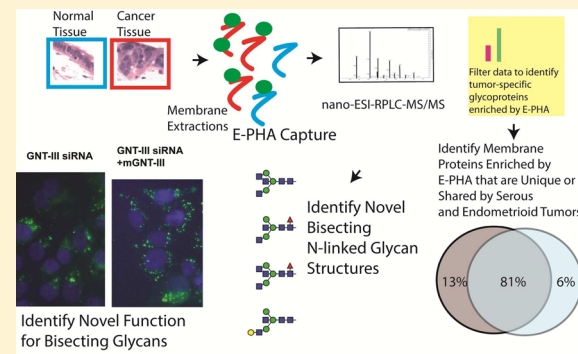
[§]Ovarian Cancer Institute, 960 Johnson Ferry Road, Atlanta, Georgia 30342, United States

^{||}University of Arkansas for Medical Sciences, Department of Biochemistry and Molecular Biology, 325 Jack Stephens Drive, Little Rock, Arkansas 72205, United States

Supporting Information

ABSTRACT: Biomarkers capable of detecting and targeting epithelial ovarian cancer cells for diagnostics and therapeutics would be extremely valuable. Ovarian cancer is the deadliest reproductive malignancy among women in the U.S., killing over 14 000 women each year. Both the lack of presenting symptoms and high mortality rates illustrate the need for earlier diagnosis and improved treatment of this disease. The glycosyltransferase enzyme GnT-III encoded by the *Mgat3* gene is responsible for the addition of GlcNAc (*N*-acetylglucosamine) to form bisecting N-linked glycan structures. GnT-III mRNA expression is amplified in ovarian cancer tissues compared with normal ovarian tissue. We use a lectin capture strategy coupled to nano-ESI-RPLC-MS/MS to isolate and identify the membrane glycoproteins and unique glycan structures associated with GnT-III amplification in human ovarian cancer tissues. Our data illustrate that the majority of membrane glycoproteins with bisecting glycosylation are common to both serous and endometrioid histological subtypes of ovarian cancer, and several have been reported to participate in signaling pathways such as Notch, Wnt, and TGF β .

KEYWORDS: biomarkers, ovarian cancer, mass spectrometry, glycoproteins, bisecting N-linked glycans, human tissue



INTRODUCTION

The discovery of biomarkers useful for the early detection of epithelial ovarian cancer (EOC) has been complicated by several factors: (i) there are different histological subtypes of EOC that have very unique genetic alterations, (ii) the tissues and serum samples available for biomarker discovery are frequently collected from patients in later stages of the disease, and (iii) the expected sensitivity and specificity required for a biomarker to detect EOC is high due to the lower disease incidence and high risk surgical interventions. Despite these obstacles, proteomic studies profiling potential biomarkers for EOC have the potential to increase our knowledge about this disease, leading to improvements in clinical disease management.

Glycoproteins account for ~80% of the proteins located at the cell surface and in the extracellular environment. Therefore, strategies to identify glycoproteins that have tumor-specific glycosylation changes could lead to the discovery of novel diagnostic and therapeutic markers. In our present study, we are targeting the neutral N-linked glycan structure known as

bisecting glycosylation that is amplified in ovarian cancer tissues, focusing on membrane proteins. Membrane proteins play pivotal roles in regulating signaling pathways, and these proteins can frequently be found both on the cell surface and in circulation due to enzyme release making them ideal potential biomarkers.

Bisecting glycosylation, added by the glycosyltransferase known as GnT-III, is normally expressed on glycoproteins in the brain and kidney.¹ The functional effects of amplified bisecting glycosylation on the growth and spread of ovarian cancer have not been determined previously. In this manuscript, we have identified membrane proteins with bisecting glycosylation from human primary endometrioid and serous ovarian cancer tissues and determined the glycan structures from these proteins using mass spectrometry methods. Functional annotation of this data demonstrates that membrane proteins with

Special Issue: Environmental Impact on Health

Received: November 12, 2014

Published: December 1, 2014

bisecting glycosylation in ovarian cancer have significant functions including: cell adhesion, control of immune responses, regulation of protein transport, and participation in signaling pathways such as Notch, Wnt, and TGF β . Also, our glycan structural analysis from primary ovarian tumor tissues demonstrates that GnT-III overexpression in human ovarian cancer produces bisected N-linked glycans that have dramatic reductions in branching and extensions and may be useful as a biomarker for the development of therapeutic and diagnostic advances.

MATERIALS AND METHODS

Materials

Biotinylated E-PHA (*Phaseolus vulgaris* erythroagglutinin) and streptavidin-HRP were obtained from Vector Laboratories (Burlingame, CA). PNGaseF was from New England Biolabs (Ipswich, MA). Chymotrypsin and sequencing grade trypsin were obtained from Promega. Vydac C18 silica columns were obtained from The Nest Group. The EGFR receptor antibody, HA antibody, 4G10 antibody, and all secondary antibodies were obtained from Santa Cruz Biotechnologies. The streptavidin-FITC, EGF-FITC, and EEA1 antibody were obtained from Invitrogen. The mouse HA-tagged GnT-III expression construct was a gift from Dr. Pamela Stanely (Albert Einstein College of Medicine). The puromycin resistance shRNA lentivirus construct was obtained from SBI System Biosciences. Fresh frozen human endometrioid ovarian cancer (EOC) tissues ($n = 3$), human serous ovarian cancer tissues ($n = 3$), normal human ovary tissues ($n = 2$), and isolated ovarian surface epithelial cells (100 mg each) were obtained from the Ovarian Cancer Institute (Atlanta, GA). Institutional review board approval for this research was obtained from the Georgia Institute of Technology, The University of Georgia, Northside Hospital (Atlanta, GA) and The University of Arkansas for Medical Sciences.

Membrane Protein Extraction, E-PHA Binding, and Peptide Preparation

Tissue or cells (100 mg) were homogenized in 10 mM Hepes pH 7.5. The slurry was placed in a Dounce glass homogenizer, and cells were lysed with 10 strokes of the large and fine pestle. The solution was incubated on ice for 1 h to continue the hypotonic cell lysis. Nuclei were removed by multiple centrifugations at 3000 rpm at 4 °C. The supernatant was placed in a Beckman ultracentrifuge tube, and the solution was centrifuged at 100 000g for 1 h at 4 °C to isolate a total membrane pellet. The pellet was rinsed and sonicated into 40 mM ammonium bicarbonate/10 mM DTT at room temperature for 2 h to reduce proteins. An equal volume of iodoacetamide (10 mg/mL) in 40 mM ammonium bicarbonate was added, and the solution was mixed by vortexing and placed in the dark for 45 min. The solution was dialyzed into 10 mM ammonium bicarbonate using Tube-O-Dialyzer membranes overnight at 4 °C. Protein concentration was measured using BCA assay, and 500 μ g of total proteins was used for E-PHA capture, while 60 μ g was digested with sequencing-grade trypsin overnight for prelectin nano-ESI-RPLC-MS/MS analysis. Sodium chloride was added to each E-PHA capture sample (final 150 mM), 5 mM calcium chloride, 5 mM magnesium chloride, and 10 μ g biotinylated E-PHA lectin prior to overnight incubation at 4 °C. Lectin-bound proteins were captured using 100 μ L of paramagnetic streptavidin particles (Promega) at 4 °C for 2 h. Beads were washed three times with 10 mM ammonium bicarbonate supplemented with salts. Proteins were eluted from beads

using 4 M urea/4 mM DTT/40 mM ammonium bicarbonate at 50 °C for 1 h. Proteins were digested with 5 μ g of sequencing-grade trypsin overnight at 37 °C. Peptides were acidified to a final of 0.1% trifluoroacetic acid and purified using C18 spin columns. Peptides were dried in a speedVac prior to resuspension in 19.5 μ L of buffer A (0.1% formic acid) and 0.5 μ L of buffer B (75% acetonitrile, 0.1% formic acid). Tryptic peptides were analyzed by nanoflow LC-MS/MS with a Thermo Orbitrap Velos mass spectrometer equipped with a Waters nanoACQUITY LC system. Tryptic peptides were separated by reverse-phase Jupiter Proteo resin (Phenomenex) on a 100 × 0.1 mm column using a nanoAcuity UPLC system (Waters). Peptides were eluted using a 120 min gradient from 98:2 to 40:60 buffer A/B ratio. Buffer A = 0.1% formic acid, 0.05% acetonitrile, buffer B = 0.1% formic acid, 75% acetonitrile. Eluted peptides were ionized by electrospray (2.0 kV), followed by MS/MS analysis using collision-induced dissociation on a Thermo LTQ Orbitrap Velos mass spectrometer. MS data were acquired using the FTMS analyzer in a profile mode at a resolution of 60 000 over a mass range of 375 to 1500 m/z . MS/MS data were collected from the top 15 peaks from each MS scan using the ion trap analyzer in centroid mode and normal mass range with normalized collision energy of 35.0 with a dynamic exclusion of two repeat counts at 30 s duration.

Permetylation and Glycan Analysis

To facilitate the analysis of oligosaccharides by MS, N-linked glycans from E-PHA captured glycoproteins were released by N-glycanase and permethylated as described previously.² Briefly, E-PHA captured glycoproteins were digested with trypsin and chymotrypsin. The resulting digests were enriched for glycopeptides prior to PNGaseF (Prozyme) treatment to release the N-linked glycans. Contaminating peptides and salts were removed using Sep-Pak C18 chromatography, and the resulting glycans were permethylated prior to analysis using a linear ion trap mass spectrometer (LTQ Orbitrap; Thermo Scientific). Detection and relative quantification of bisecting N-linked glycan structures were carried out by using the total ion mapping (TIM) function of the Xcalibur software package version 2.0 (Thermo Fisher Scientific) as described previously.³ The TIM profiles were initially filtered with neutral loss of terminal HexNAc (Δ mass, 260 (1+), 130 (2+), and 86.7 (3+)) to assess the presence of bisecting N-linked glycan structures. N-glycan structures carrying terminal HexNAc were further subjected to manual MSn analysis to determine bisecting N-linked glycan structures.

Proteomic Data Analysis

Raw peptide data were converted to mzXML, and MS/MS spectra were searched against the International Protein Index (IPI) human database (IPI.HUMAN.v.3.71) using MyriMatch.⁴ All unambiguous identifications matched to multiple peptide sequences were excluded. Proteins identified required 2+ peptides and were grouped using IDPicker software.⁵ IDPicker incorporates searches against a separate reverse database, probability match from MyriMatch, and DeltCN scores to achieve a false-discovery rate of <5%. Information on MyriMatch and IDPicker can be found at <http://fenchurch.mc.vanderbilt.edu/software.php>. Variance for membrane protein extractions and E-PHA capture between normal and tumor tissues were calculated by measuring the number of peptides identified for proteins that adhere to E-PHA from membrane extractions in a non-glycan-dependent manner such as HSPA2 and RPL9. Values observed for tumor tissues for HSPA2 (CV 0.63/8 peptides) and RPL9 (CV 1.36/4 peptides). Values observed for normal tissues

Table 1. Membrane Proteins Enriched by E-PHA Capture from Ovarian Carcinoma Tissues^a

IPI ^c	gene code	mol wt (kDa)	% coverage	protein name	unique peptides	subtype	localization	function	HPA/staining ^b
IP100478003	A2M	163	40	alpha 2-macroglobulin	39	both	extracellular membrane	immune transport	
IP100291373	ABCD1	81	4.5	ATP-binding cassette sub family D angiotensin-converting enzyme, CD143	2	both	endo membrane	enzyme	low (3/11)
IP100437751	ACE	149	3.2	disintegrin and metalloproteinase domain-containing protein 10, CD156c	4	endo	endo membrane	enzyme	low/med (5/1 of 11)
IP100013897	ADAM10	84	4	anterior gradient protein 2 homologue	2	endo	extracellular membrane	protein binding	high (3/10)
IP100021812	AGR2	19	20	CD166 antigen	3	both	extracellular membrane	cell adhesion	high/med/low (2/3/6 of 12)
IP100015102	ALCAM	65	5.6		3	both	membrane		low (1/11)
IP100004457	AOC3	84	17.3	membrane primary amine oxidase	7	both	membrane	enzyme	low (3/11)
IP100022391	APCS	24	31.8	serum amyloid P-component	6	both	extracellular membrane	protein binding	high/med/low (1/6/1 of 9)
IP100031131	APMAP	46	18	adipocyte plasma membrane-associated protein	7	both	membrane	enzyme	high/med/low (1/12)
IP100021841	APOA1	29	47	apolipoprotein A-I	13	both	extracellular membrane	transport	low (1/12)
IP100021842	APOE	36	29	apolipoprotein E	7	both	membrane	transport	high/med/low (3/3/3 of 12)
IP100418446	ASAH1	43	21	acid ceramidase	8	both	lysosome	enzyme	med/low (4/5 of 12)
IP100418431	ASPN	44	28	asporin	10	both	extracellular	signaling	high/med/low (1/5/1 of 12)
IP100006482	ATP1A1	35	25	sodium/potassium-translocating ATPase subunit alpha-1	19	both	membrane	transport	high/med/low (5/6/1 of 12)
IP100002406	BCAM	67	24	basal cell adhesion molecule, CD239	10	both	membrane	cell adhesion	high/med/low (6/4/2 of 12)
IP100218200	BCAP31	27	23	B-cell receptor-associated protein 31	8	both	membrane, ER	transport	med (12 of 12)
IP100010790	BGN	41	28	biglycan	6	both	extracellular membrane	signaling	low (2/11)
IP100019906	BSG	29	26	basigin (CD147)	5	both	membrane	signaling	high/med/low (3/5/3 of 12)
IP100026241	BST2	23	13.8	bone marrow stromal antigen, CD317	2	ser	membrane, GPI	immune	high/med/low (3/8/1 of 12)
IP100418163	C4B	192	16	complement component 4B	24	both	membrane	immune	med/low (3/1 of 12)
IP100029260	CD14	40	15	monocyte differentiation antigen	4	both	membrane, GPI	immune	
IP100104074	CD163	12.5	9.5	scavenger receptor cysteine-rich type 1 protein M130	8	both	membrane	immune	
IP100374740	CD47	35	6	leukocyte surface antigen CD47	2	both	membrane	signaling	high/med/low (6/2/2 of 11)
IP100111302	CD59	14	70	CD59 glycoprotein	8	both	membrane, GPI	immune	med/low (1/3 of 11)
IP100022933	CD74	33	16.9	HLA DR antigen	3	both	membrane	immune	high/med (7/4 of 11)
IP100215997	CD9	25	15.3	CD9 antigen	2	both	membrane	cell adhesion	high/med/low (3/8/1 of 12)
IP100024046	CDH13	83	3.4	cadherin-13	2	ser	membrane, GPI	cell adhesion	high (12 of 12)
IP100000513	CDH1	90	5	E-cadherin	3	endo	membrane	cell adhesion	med/low (6/4 of 10)
IP100019591	CFB	140	10	complement factor B	10	both	membrane	immune	high/med/low (5/2/3 of 12)
IP100141318	CKAP4	66	47	cytoskeleton-associated protein 4	27	both	membrane	cell proliferation	med/low (3/2/10)
IP100291262	CLU	52	22	clusterin	9	both	membrane	immune	
IP100297646	COL1A1	139	10	collagen alpha-1(I) chain	12	both	extracellular	signaling	low (1/9)
IP100017292	CTNNB1	85	15.5	beta-catenin	11	both	membrane	signaling	high/med (7/4 of 11)

Table 1. continued

IPI ^c	gene code	mol wt (kDa)	% coverage	protein name	unique peptides	subtype	localization	function	HPA/staining ^b
IP100295741	CTSB	38	18	cathepsin B	4	both	lysosome	enzyme	high/med/low (1/5/1 of 11)
IP100111229	CTSD	44	24	cathepsin D	7	both	lysosome	cell adhesion	high/med/low (1/3/7 of 12)
IP100002714	DKK3	38	7.5	Dickkopf-related protein	2	endo	extracellular	signaling	med/low (2/5 of 12)
IP100029658	EFEMP1	55	20	EGF-containing fibulin-like extracellular matrix protein 1 (fibulin-3)	7	both	extracellular	cell adhesion	high/med/low (1/2 of 12)
IP100018274	EGFR	134	2.6	epidermal growth factor receptor	2	ser	membrane	signaling	med/low (1/2 of 12)
IP100013079	EMILIN	106	30	emilin-1	28	both	extracellular	cell adhesion	low (1/ of 12)
IP100219625	ENG	68	13	endoglin, CD105	6	ser	membrane	cell adhesion	high/med (7/5 of 12)
IP100296215	EPCAM	21	27	epithelial cell adhesion molecule, CD326	3	both	membrane	cell proliferation	low (11/ of 12)
IP100298105	EPHA3	110	4.2	ephrin receptor	3	endo	GPI	signaling	med (1/ of 12)
IP100010951	EPHX1	53	33	epoxide hydrolase	14	both	membrane, ER	enzyme	low (10/ of 10)
IP100409635	ESYT2	98	8	extended synaptotagmin-2	6	ser	membrane	protein binding	low (1/ of 11)
IP100382428	FBLN5	60	14	fibulin 5	7	both	extracellular	cell adhesion	low (1/ of 12)
IP100328113	FBN1	312	35	fibrillin-1	75	both	membrane	signaling	med (1/ of 11)
IP100294578	GGT2	77	15	gamma-glutamyltransferase 2	7	both	membrane	enzyme	med/low (1/2 of 11)
IP100002243	GGTS	62	11	gamma-glutamyltransferase 5	5	both	membrane	enzyme	high/med (11/1 of 12)
IP100016801	GLUD1	61	38	glutamate dehydrogenase 1	17	both	membrane, mito	cell adhesion	low (3/ of 12)
IP100001592	GPNMB	64	4.4	transmembrane glycoprotein NMB	2	endo	membrane	signaling	med/low (2/1/ of 9)
IP100004901	GPRC5C	48	5	G-protein coupled receptor family C group 5 member C	3	endo	membrane	protein binding	high/med/low (1/4/ 4 of 11)
IP100024284	HSPG2	468	3.1	basement membrane heparin sulfate proteoglycan	10	both	membrane	transport	high/med/low (3/6/ 3 of 12)
IP100289819	IGF2R	274	1.8	insulin-like growth factor receptor 2	4	both	membrane	signaling	high/med/low (1/4/ 4 of 11)
IP100217563	ITGB1	88	22	integrin beta-1, CD29	15	both	membrane	transport	high/med/low (3/6/ 3 of 12)
IP100291792	ITGB2	85	16	integrin beta-2, CD18	10	both	membrane	signaling	low (6/ of 10)
IP100032328	KNG1	71	8	kininogen-1	4	both	extracellular	protein binding	med (1/ of 12)
IP100334532	LICAM	140	1.9	neural cell adhesion molecule L1, CD171	2	endo	membrane	cell adhesion	med/low (3/5/ of 12)
IP100884105	LAMP1	45	7	lysosome-associated membrane glycoprotein 1, CD107a	3	both	membrane	transport	high/med/low (2/9/1/ of 12)
IP100026530	LMAN1	57	24	ERGIC-53	9	both	membrane	transport	high/med/low (6/4/ 1 of 12)
IP100009950	LMAN2	40	6	vesicular integral-membrane protein VIP36	2	endo	membrane	transport	low (1/1/ of 11)
IP100020557	LRP1	504	5.4	proline-rich lipoprotein receptor-related protein 1, CD91	20	both	membrane	signaling	low (1/ of 10)
IP100024292	LRP2	522	2.5	low-density lipoprotein receptor-related protein 2	10	both	membrane	signaling	low (3/10)
IP100301202	MAGT1	28	8	magnesium transporter 1	2	endo	membrane	transport	high/med (2/10/ of 12)
IP100328156	MAOB	46	20	amine oxidase [flavin-containing] B	9	both	membrane	enzyme	high/med/low (3/4/ 5 of 12)
IP10016334	MCAM	71	8	cell surface glycoprotein MUC18	4	both	membrane	cell adhesion	med/low (1/1/ of 11)
IP100022621	MFAP2	21	12	microfibril-associated glycoprotein 2	2	both	extracellular	cell adhesion	low (1/ of 10)
IP100022336	MFGE8	43	17	lactadherin	5	both	membrane	cell adhesion	low (3/ of 12)
IP100029046	MLEC	32	19	malestin	4	both	membrane, ER	protein binding	low (3/ of 12)
IP100247063	MME	85	9.4	nephrin, CD10	6	endo	membrane	enzyme	

Table 1. continued

IPI ^c	gene code	mol wt (kDa)	% coverage	protein name	unique peptides	subtype	localization	function	HPA/staining ^b
IP100027509	MMP9	78	6.5	matrix metalloproteinase 9	3	endo	extracellular membrane	enzyme	med/low (7/3/ of 10)
IP100013955	MUC1	60	8	mucin 1	4	endo	membrane	cell adhesion	high/med/low (6/3/2 of 11)
IP100021048	MYOF	234	18	myoferin	29	both	membrane	transport	high/med/low (2/6/1 of 10)
IP100021983	NCSTN	78	4.5	nicastrin	2	ser	membrane	signaling	high/med/low (3/4/5/ of 10)
IP100329352	NOMO3	139	9	nodal modulator 3	9	both	membrane	signaling enzyme	high/med/low (3/4/5/ of 12)
IP100465159	NOTUM	49	11	protein notum homology	4	endo	extracellular membrane,		
IP100009456	NTSE	63	16	S'-nucleotidase, CD73	8	both	GPI	enzyme	high/med/low (3/4/5/ of 12)
IP100022255	OLF M4	57	57	olfactomedin-4	9	endo	extracellular	cell adhesion	cell adhesion
IP100024621	OLF M3	43	12	olfactomedin-3	4	ser	extracellular	cell adhesion	low (5/ of 12)
IP100013569	PAPP A2	198	3.3	pappalysin-2	4	both	extracellular	enzyme	med/low (2/2/ of 11)
IP100384280	PCYOX1	56	14	prenylcytsteine oxidase 1	6	both	lysosome		
IP100220739	PGRMC1	22	34	membrane-associated progesterone receptor component 1	5	both	membrane	protein binding	med/low (6/6/ of 12)
IP100004573	PIGR	83	16	polymeric immunoglobulin receptor	8	both	membrane	protein binding	high (4/11)
IP100019580	PLG	90	24	plasminogen	14	both	extracellular	enzyme	low (2/ of 12)
IP100299116	PODXL	55	8.6	podocalyxin-like protein	4	both	membrane	cell adhesion	med (2/ of 12)
IP100007960	POSTN	93	20	periostin	12	both	extracellular	cell adhesion	
IP100020987	PRELP	44	33	proargin	10	both	extracellular	protein binding	low (2/ of 12)
IP100012540	PROM1	97	2.7	proninin-1, CD133	2	endo	membrane	signaling	high/med/low (3/3/3/ of 12)
IP100006865	SEC22B	25	26	vesicle-trafficking protein SEC22b	4	both	membrane	transport	
IP100553177	SERPINA1	40	17	alpha-1-antitrypsin	5	both	extracellular	protein binding	low (1/ of 10)
IP100006114	SERPINF1	46	16	pigment-epithelium derived factor	6	endo	extracellular	cell proliferation	med/low (2/2/ of 12)
IP100019385	SSR4	42	23	translocon-associated protein subunit delta precursor	3	both	membrane	transport	high/med/low (1/10/1/ of 12)
IP100219682	STOM	31	40	erythrocyte band 7 integral membrane protein	8	both	membrane	transport	
IP100296099	THBS1	129	26	thrombospondin-1	25	both	extracellular	cell adhesion	high/med (5/6/ of 12)
IP100018769	THBS2	129	28	thrombospondin-2	24	both	extracellular	cell adhesion	med/low (4/2/ of 10)
IP100022892	THY1	16	27	Thy-1 membrane glycoprotein, CD90	3	both	membrane, GPI	signaling	med (1/ of 12)
IP100640293	TIMP3	24	34	metalloproteinase inhibitor 3	6	both	extracellular	protein binding	high/med/low (2/5/1/ of 11)
IP100028055	TMED10	21	13	transmembrane emp24 domain-containing protein 10	2	both	membrane	transport	high/med/low (1/8/3/ of 12)
IP100298362	TNFRSF11B	46	9.4	tumor necrosis superfamily receptor	3	both	extracellular	signaling	high/med/low 3/6/3/ of 12)
IP100554617	TPP1	61	7	tripeptidyl-peptidase 1	3	both	lysosome	enzyme	med/low (1/1/ of 10)
IP100298971	VTN	54	23	vitronectin	9	both	extracellular	cell adhesion	

^aTwo independent peptide matches required from two separate samples. Tumor-specific E-PHA enrichment required 1.5 times increase in spectral counts and peptide abundance in tumor tissues compared with nonmalignant tissues. ^bHuman Protein Atlas ovarian cancer tissue staining data (www.proteinatlas.org). ^cInternational Protein Index Database.

HSPA2 (CV 0.71/7 peptides) and RPL9 (CV 1.4/4 peptides). These results indicate a $12 \pm 1.0\%$ variance between normal and tumor samples due to processing. This variance is well below the 1.5 times or 150% increase in peptides and spectral counts we have established as criteria to be considered as a glycoprotein with tumor-specific E-PHA reactivity.

Biological Functional Annotation

Proteins in Table 1 were uploaded to DAVID 2009 (the Database for Annotation, Visualization and Integrated Discovery) for analysis.

ShRNA Lentivirus Cloning, Lentivirus Production, Cell Transduction, and Cell Proliferation Assays

Two target sequences were tested for GnT-III suppression in human cells. One sequence gave >75% reduction in GnT-III expression in human ovarian adenocarcinoma cells (NM_002409, 5' ctacgaccgggttccactac). Briefly, the target sequence along with restriction site linkers and shRNA loop sequence was cloned into the pSIH-H1shRNA vector (System Biosciences). Lentivirus was produced in 293TN cells, and OVCAR3 cells were transduced as previously described.⁶ OVCAR3 cells stably expressing GnT-III siRNA target sequence were transfected transiently with HA-tagged mouse GnT-III cDNA expression plasmid (gift from Pamela Stanley) or empty cDNA vector. Subconfluent cells were serum-starved for 24 h prior to the addition of 25 ng/mL EGF for 24 h. Cell proliferation was measured using the CellTiter Aqueous One solution (Promega) according to the manufacturer's recommendations and absorbance was read at 490 nm. The \pm SEM represents results from three separate experiments.

Microscopy

E-PHA Lectin Staining. Cells were grown to subconfluence in chamber slides before fixing in 3% formaldehyde/1× phosphate buffered saline (PBS) for 10 min. Cells were blocked using 1% bovine serum albumin (BSA)/1XPBS-0.2% tween-20 (PBST) prior to the addition of biotin-labeled E-PHA (Vector Laboratories) diluted 1:300 in 1% BSA/1XPBST. Bound lectin was detected using fluorescein-tagged streptavidin (Invitrogen) diluted 1:500 in 1% BSA/1XPBST.

EGF Internalization. Cells were grown to subconfluence and serum starved prior to analysis. Cells were placed on ice for 1 h in the presence of fluorescein tagged EGF (50 ng/mL) (Invitrogen). Cells were placed back at 37 °C for 30 min before the removal of unbound EGF with ice-cold 20 mM acetic acid/0.5 M NaCl. Cells were fixed prior to detection of early endosomes using anti-EEA1 (1:400) (Invitrogen), followed by rhodamine antimouse IgG (1:250). Nuclei were visualized using Dapi counterstain.

RESULTS

Glycoproteins at the Cell–Cell Boundary of Ovarian Cancer Cells Are Bound by E-PHA in a GnT-III-Dependent Manner

In previous studies we have used the plant lectin E-PHA (*Phaseolus vulgaris* Erythroagglutinin) to capture soluble or extracellular glycoproteins with bisecting glycosylation from human ovarian cancer tissues due to the elevation of this form of glycosylation in human epithelial EOC.^{7,8} In this study, we are comparing the analysis of both serous and endometrioid ovarian cancer, the two most abundant histological subtypes of EOC, focusing on the identification of glycoproteins located in the membrane fraction that have tumor-specific bisecting glycosylation. Bisecting glycosylation is amplified in ovarian cancer

due to increased expression of the glycosyltransferase GnT-III.^{7,9} Therefore, to explore the localization of glycoproteins with bisecting glycosylation and validate the specificity of E-PHA for this glycan structure, we have created cell lines using the human ovarian adenocarcinoma cell line known as OVCAR3 that express either a control shRNA sequence that targets no human gene (control siRNA) or a GnT-III shRNA target sequence (GnT-III siRNA). Constitutive expression of the GnT-III siRNA reduced the expression of GnT-III by >75% compared with control siRNA (Figure 1A). E-PHA binding in OVCAR3 cells

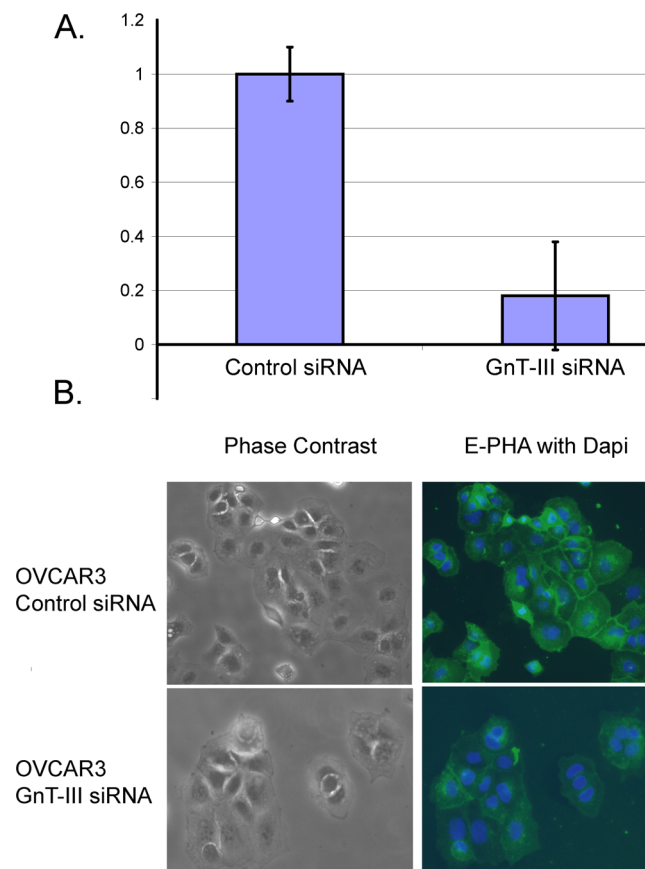


Figure 1. E-PHA binds bisecting glycans in a GnT-III dependent manner. (A) Real-time PCR measurement of GnT-III mRNA levels in OVCAR3 human ovarian cancer cells expressing control siRNA or GnT-III siRNA. GnT-III levels were normalized to RPL4 and the control siRNA level was set to 1.0 for comparison; error bars represent the mean \pm SE for triplicate measurements. (B) E-PHA staining of glycoproteins with bisecting glycosylation in OVCAR3 cells; nuclei are stained with DAPI, magnification 20 \times .

stably expressing the control siRNA is strong, localized to the cell–cell junctions, indicating a concentration of glycoproteins at the cell periphery with bisecting glycosylation. The cell boundaries of OVCAR3 cells stably expressing GnT-III siRNA are not visible, indicating a loss of E-PHA accumulation and a reduction of bisecting glycosylation (Figure 1B). Therefore, E-PHA binding to glycoproteins in OVCAR3 cells requires the expression of GnT-III, and glycoproteins with bisecting glycosylation are concentrated at the cell periphery.

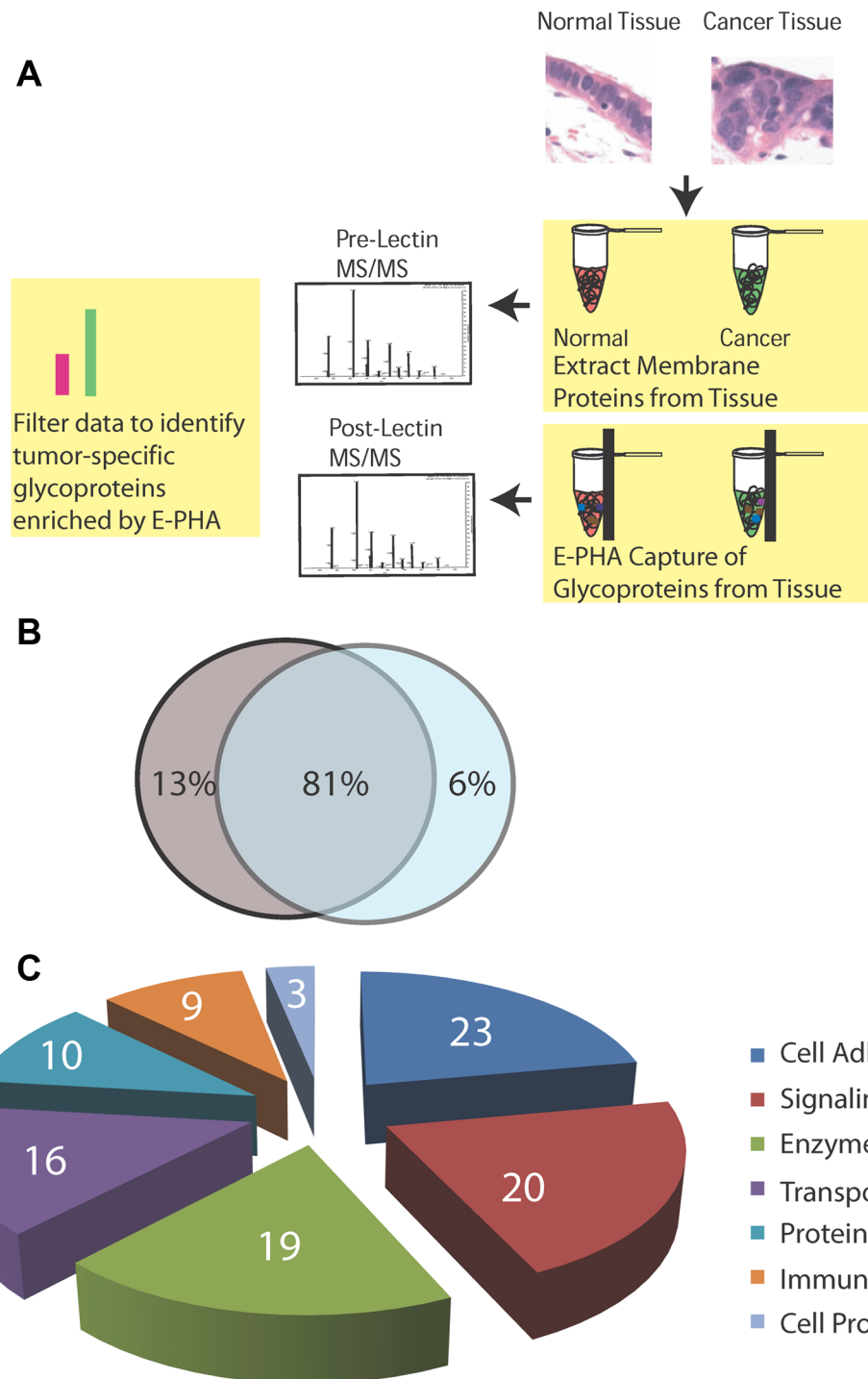


Figure 2. (A) Schematic flow of glycoproteomic experiments. Membrane proteins were analyzed by nanoflow-ESI-RPLC-MS/MS before E-PHA capture to verify equivalent protein quality and quantity. Biotinylated E-PHA was added to membrane extracted proteins, and glycoproteins with bisecting glycans were captured using streptavidin magnetic resin prior to nanoflow-ESI-RPLC-MS/MS. Membrane glycoproteins enriched in tumor tissues relative to nonmalignant tissues by E-PHA capture by at least 1.5 times or 150% by spectral counts were identified and are listed in Table 1. (B) Venn diagram showing the percentage of glycoproteins in Table 1 from endometrioid only (13% purple), serous only (6% blue), or shared (81% blue/purple). (C) Functional annotation of E-PHA enriched membrane glycoproteins using DAVID 2009.

E-PHA Capture of Tumor-Specific Glycoproteins from Serous and Endometrioid Ovarian Cancer Tissues Reveals Common Glycoprotein Targets for the Two Most Common Types of EOC

Fresh frozen tissue samples (Supplementary Table 1 in the Supporting Information) from EOC ($n = 3$), serous ovarian cancer ($n = 3$), nonmalignant ovary ($n = 2$), or isolated

nonmalignant ovarian surface epithelial cells ($n = 1$) were each subjected to membrane protein isolation and E-PHA lectin capture. A diagram of the extraction and analysis scheme for glycoproteomics is shown in Figure 2A. Comparison analysis of each membrane extracted sample before and after E-PHA capture enabled the identification of glycoproteins that are potential acceptors for bisecting glycosylation. Glycoproteins

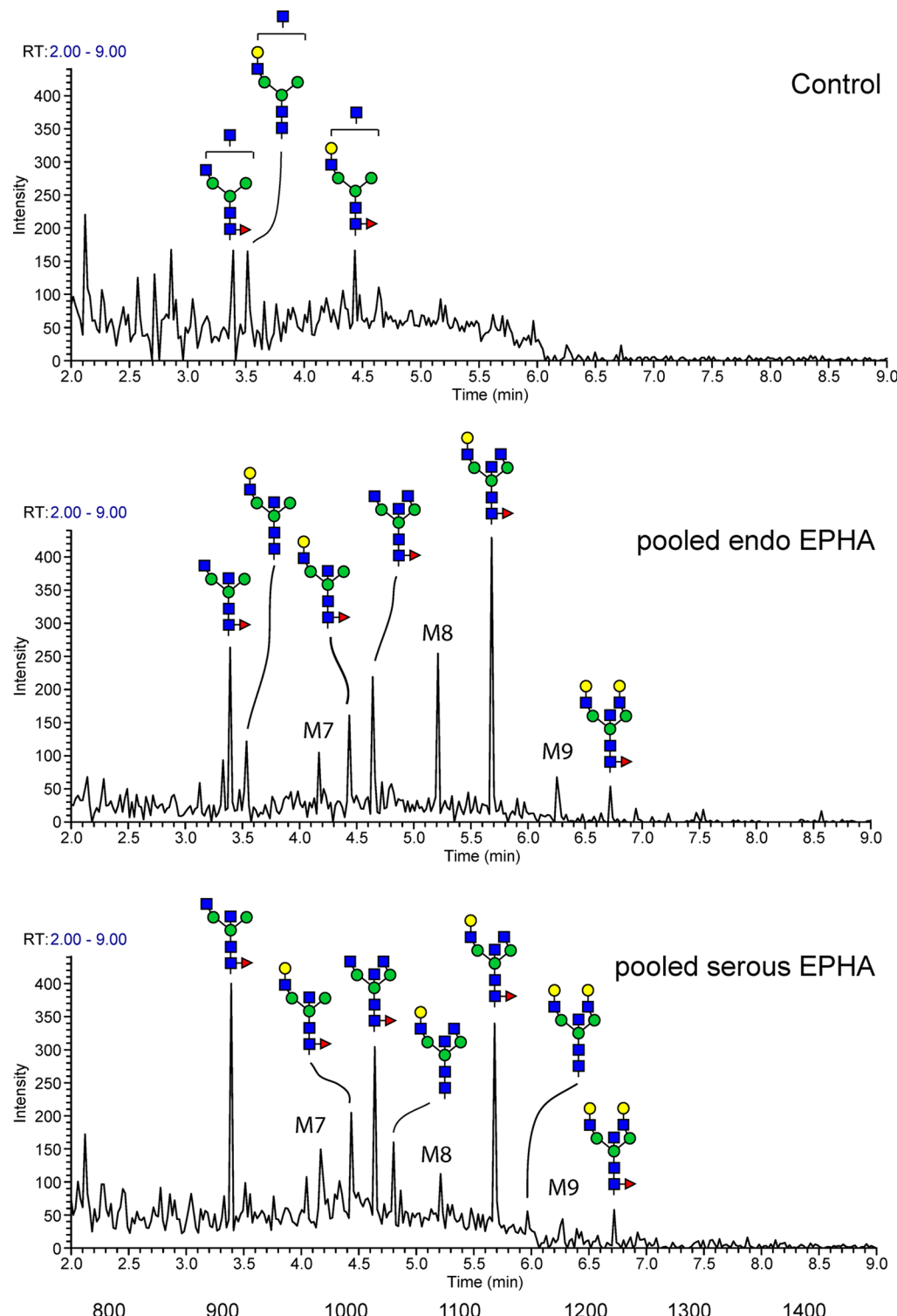


Figure 3. Prevalence of unique bisecting N-linked glycan structures in ovarian carcinoma tissues. PNGaseF released N-linked glycan structures from glycoproteins enriched by E-PHA capture. Glycans were released from pooled E-PHA captured glycoproteins from endometrioid ($n = 3$), serous ($n = 3$), or total membrane proteins from nonmalignant control surface epithelial cells ($n = 1$). TIM profile was filtered with neutral loss of HexNAc and bisecting N-linked glycan structures were identified by MS_n analysis manually. Peaks labeled M7, M8, and M9 indicate high mannose type N-linked glycans.

that were enriched following E-PHA capture by at least 1.5 times (150% by spectral counts) in tumor tissues relative to nonmalignant controls are listed in Table 1. In Table 1, we provide Human Protein Atlas (HPA)¹⁰ antibody immunohistochemistry staining data (for ovarian cancer tissues) for each E-PHA enriched glycoprotein. Over 80% of the glycoproteins in

Table 1 have positive antibody immunohistochemistry staining in ovarian carcinoma tissues (data from the HPA annotated in Table 1).¹⁰ The majority (81%) of glycoproteins enriched by E-PHA are present in both histological subtypes of EOC, suggesting that the glycosylation changes on these proteins are important for the survival and growth of ovarian cancer cells

(Figure 2B). The overall functional annotation (Figure 2C) of glycoproteins enriched by E-PHA capture reveals that the largest functional categories are cell adhesion, regulation of signaling, enzymatic functions, and control of protein transport (Figure 2C). Several glycoproteins have reported activities in the Notch^{11–15} (LRP2, POSTN, THBS1, THBS2, MFAP4, OLFM4, NCSTN), TGF β ^{16,17} (ASPN, FBN1, ENG), and Wnt¹⁸ (COL1A1, CTNNB1) signaling pathways. These pathways are all implicated in control of cancer stem cell populations.

E-PHA Captured Glycoproteins from Serous and Endometrioid Ovarian Cancer Share a Unique Truncated N-Linked Glycan Structure Not Found in Control Nonmalignant Samples

The membrane-extracted proteins from endometrioid and serous ovarian tissues were subjected to PNGaseF treatment following E-PHA capture. Membrane proteins extracted from nonmalignant ovarian surface epithelial cells have low levels of binding to E-PHA; therefore, equivalent levels of total membrane protein were used for the release of N-linked glycans. The N-linked glycans were released from trypsin and chymotrypsin digests using PNGaseF before permethylation and analysis using mass spectrometry methods. We have identified nine very unique and unusual bisecting N-linked glycan structures that are present in both endometrioid and serous EOC tissues (Figures 3 and 4) that were not observed in control nonmalignant ovarian epithelial cells. The full MS reveals the presence of abundant high mannose glycan structures (Supplemental Figure 1 in the Supporting Information) that are marked with asterisks in Figure 3. MS6 analysis was necessary to confirm the presence of the bisecting glycan structures (Supplemental Figures 2–4 in the Supporting Information). The fragment ion observed at m/z 444 for MS6 clearly demonstrates the presence of the bisected mannose, of which three of the hydroxyl groups were substituted with three HexNAc (Supplemental Figures 2–4 in the Supporting Information). Although, some of the bisecting N-linked glycan structures contain isobaric forms of N-glycans capped with terminal HexNAc, which demonstrates a specific fragment ion at m/z 458 for MS6 (Supplemental Figure 2 in the Supporting Information). Thus, the sequential MS n approach using permethylated N-glycans effectively discriminates bisecting N-glycan structures from other N-glycans with terminal HexNAc. The most prevalent bisecting N-linked structures are shown on the TIM chromatogram (Figure 3). These structures are dramatically truncated with minimal branching with reductions in distal galactose and sialic acid modifications. Most of the bisecting N-linked glycans also have core fucosylation, another neutral N-linked glycan structure known to be amplified in EOC.^{7,19} The unusual lack of branched glycans with the presence of core fucosylation may represent a biomarker useful for the development of future therapeutic and diagnostic applications.

Novel Role for Bisecting Glycosylation in Protein Transport

Our glycoproteomic analysis of E-PHA captured membrane glycoproteins from EOC has led to the identification of potential functions that bisecting glycosylation changes may impact. Several proteins enriched by E-PHA have potential functions in the control of protein transport (BCAP31, LMAN1, LMAN2, LRP2, MYOF, SEC22B, SSR4, and TMED10). To explore this area of functional significance further, we exposed the OVCAR3 cell lines, control siRNA, or GnT-III siRNA to fluorescently tagged EGF to track the transport of receptors that receive bisecting glycosylation and bind EGF, such as EGFR. EGF was

	Theoretical mass [M+2Na] ²⁺	Observed mass [M+2Na] ²⁺
	964.98	965.00
	929.45	929.50
	1052.02	1052.07
	944.46	944.51
	1067.03	1067.03
	1169.08	1069.06
	1031.50	1031.55
	1154.07	1154.12
	1256.12	1256.17

Figure 4. Bisecting N-linked glycan structures identified from human endometrioid and serous EOC. Bisecting structures identified from endometrioid and serous ovarian cancer tissues by MS n analysis are summarized. Represented glycan structures are in accordance with the guidelines from the Consortium for Functional Glycomics (CFG): blue square, N-acetylglucosamine (GlcNAc); green circle, mannose (Man); yellow circle, galactose (Gal); red triangle, fucose (Fuc).

internalized in both cells; however, in control cells, the EGF is distributed to several intracellular vesicles, and in GnT-III siRNA cells, the EGF is primarily localized in a perinuclear compartment (Figure 5). EGF is active in the cells demonstrated by the ligand-induced phosphorylation observed (Supplementary Data in the Supporting Information, Figure 5, last panel). The early endosomal marker EEA1 also displays a change in intracellular localization in GnTIII siRNA cells compared with control cells. These results suggest that bisecting glycosylation is promoting transport of certain proteins in ovarian cancer cells. To confirm that this protein transport change in GnT-III siRNA cells is due to bisecting glycosylation, we show that we can rescue this defect with the expression of mouse GnT-III in GnT-III siRNA stable OVCAR3 cells. Mouse GnT-III is not targeted by our constitutively expressed human GnT-III shRNA target sequence. Stable GnT-III siRNA OVCAR3 cells were transiently transfected with full-length mouse GnT-III fused to an HA-tag. Immunofluorescence microscopy demonstrates that cells transiently transfected show positive E-PHA staining (green, FITC, Figure 6A)) and positive HA-tag staining (red, rhodamine, Figure 6A), indicating that the mouse GnT-III is active in human cells. Introduction of the mouse GnT-III gene into

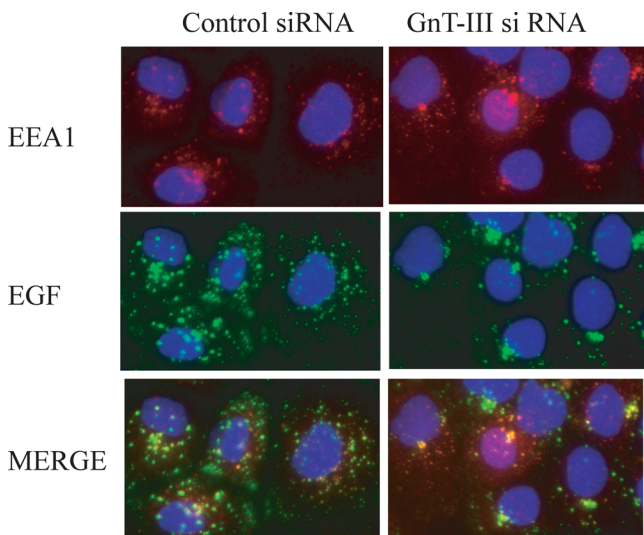


Figure 5. Protein transport is impaired in GnT-III siRNA cells. (A) OVCAR3 control siRNA cells and GnT-III siRNA cells were serum-starved prior to incubation with fluorescein-EGF (50 ng/mL) for 1 h on ice. Cells were placed in a 37 °C incubator for 30 min prior to removal of EGF that was not internalized by an acid wash. Cells were fixed and stained using an EEA1 monoclonal antibody. Nuclei are stained with DAPI, magnification 40×.

OVCAR3 cells stably expressing GnT-III siRNA can rescue the transport of EGF-bound glycoproteins (Figure 6B). Fluorescent EGF and rhodamine-stained EEA1 are transported into different intracellular vesicles in rescued cells (Figure 6B top panel), while EGF and EEA1 show stalled movement in a perinuclear compartment without rescue in the GnT-III siRNA cells without mouse GnT-III (Figure 6B, bottom panel). These experiments confirm a novel role for GnT-III expression and therefore bisecting glycans in promoting vesicular transport in human ovarian adenocarcinoma cells. Downstream signaling induced by EGF is suppressed in GnT-III siRNA cells (Supplementary Data in the Supporting Information, Figure 6). OVCAR3 cells stably expressing GNT-III siRNA have reduced basal proliferation and show no change in cell proliferation following EGF addition (Figure 6C). Transfection of mouse GNT-III increases basal cell proliferation and restores the proliferation response to EGF (Figure 6C). These data indicate that GNT-III expression and bisecting glycosylation promote the vesicular transport and activity of EGF-bound receptors such as EGFR.

■ DISCUSSION

The mechanisms that lead to overexpression of GnT-III in ovarian cancer may involve epigenetic mechanisms.⁹ A recent study of human ovarian cancer and nonmalignant ovarian epithelial cell lines demonstrated that the *Mgat3* gene could be induced following treatment with an inhibitor of DNA methyltransferase. These results provide strong evidence that the increased expression of *Mgat3* transcripts in ovarian cancer may be due to epigenetic dysregulation of hypermethylation.

The normal functional roles of bisecting glycans on glycoproteins in the kidney and brain are not well understood. The overexpression of GnT-III in ovarian cancer offers an opportunity to learn more about this form of glycosylation and discover new mechanisms that contribute to ovarian tumor growth.

We have discovered a new function for GnT-III expression and bisecting N-linked glycosylation in promoting protein transport. Suppression of GnT-III expression in the human ovarian cancer cell line OVCAR3 results in a dramatic change in the intracellular localization of EGF bound receptors. We have confirmed that EGFR is glycosylated by GnT-III in OVCAR3 cells (Supplementary Data in the Supporting Information, Figure 5, top panel). EGF was capable of activating the EGFR receptor, and there are no differences in EGFR autophosphorylation levels between control siRNA and GnT-III siRNA OVCAR3 cells (Supplementary Figure 5 in the Supporting Information), suggesting that receptor dimerization and endocytosis are not influenced by bisecting glycosylation. However, the transport of vesicles containing EGF bound receptor is slowed in cells with reduced GnT-III expression, allowing the EGF to accumulate in a perinuclear compartment. The accumulation of EGF-bound receptor in this perinuclear compartment reduces downstream EGF-induced signaling (Supplementary Data in the Supporting Information, Figure 6) and inhibits proliferative responses to EGF (Figure 6C). Our ability to rescue the transport and activity of EGF-bound receptors with the expression of mouse HA-GnT-III (Figure 6A–C) supports a role for GnT-III expression and bisecting glycosylation as a factor promoting growth factor receptor transport and activity. Our glycoproteomic analysis from ovarian cancer tissues also supports a role for bisecting glycans in protein transport as several proteins with known transport functions are enriched by E-PHA. Therapeutic strategies to block GnT-III expression, enzymatic activity, or growth factor receptor interactions with transport proteins may be new avenues to reduce ovarian cancer cell responses to growth factor ligands by slowing the movement of receptors within the cell.

The unusual bisecting N-linked glycan structures identified for both endometrioid and serous EOC subtypes are an important discovery that may lead to the development of antibodies or strategies to target ovarian cancer cells. The prevalence and similarity of these glycan structures for both histological subtypes of ovarian cancer indicate an importance for this glycan structure in the development and survival of ovarian carcinoma cells. Also, the lack of these structures in nonmalignant tissues and cells supports the use of these structures as potential biomarkers. A recent glycomics analysis of all N-linked glycan structures for membrane glycoproteins isolated from ovarian cancer and nonmalignant ovarian cell lines also found the presence of bisecting structures specific to malignant cells.⁹ GnT-III expression and bisecting glycosylation have been reported to compete with branching enzymes such as GnT-V, reducing tumor growth for cancers with elevated GnT-V expression such as breast cancer.²⁰ However, in ovarian cancer cells there is no competition with GnT-V, and the bisecting glycan structure has a growth promoting role. Furthermore, the truncated glycan structures found on bisecting N-linked glycans released from ovarian cancer tissues have not been observed in analysis of bisecting N-linked glycan structures isolated from nonmalignant cell types such as HEK293 and CHO.^{21,22} These results indicate that there may be additional changes in Golgi transport or other as yet unknown factors in ovarian cancer that may contribute to the production of these unusual glycan structures.

Several of the extracellular glycoproteins identified following the stringent membrane isolation procedures (THBS1, THBS2, LRP2, POSTN) are adhesive glycoproteins with reported functions as noncanonical regulators of the Notch signaling pathway.¹¹ The extraction of these proteins with membrane

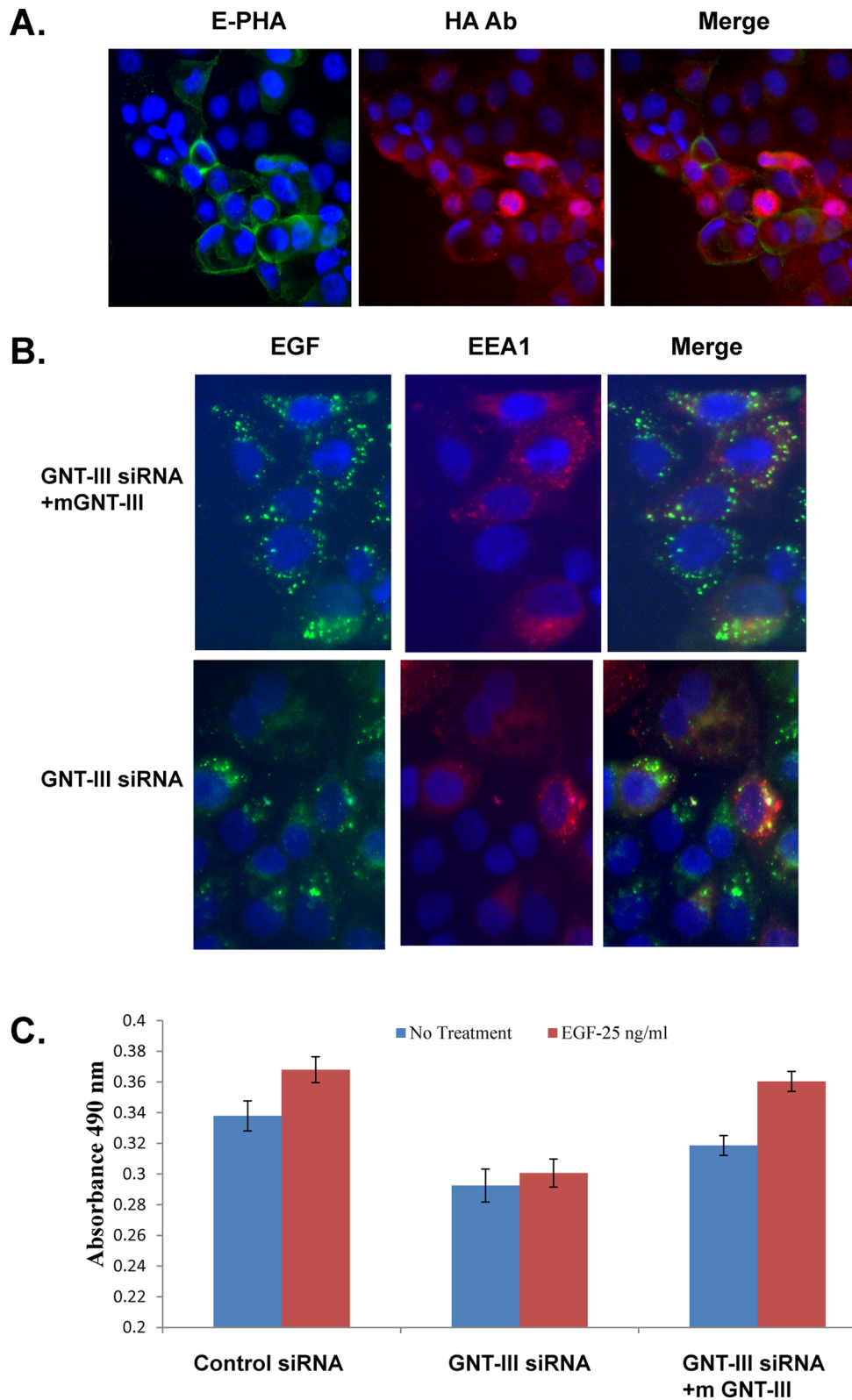


Figure 6. Protein transport and response to EGF is restored with mouse GnT-III expression. (A) OVCAR3 cells expressing GnT-III siRNA constitutively were transiently transfected with mouse HA-GnT-III (gift from Pamela Stanley). Cells expressing mouse HA-GnT-III show positive E-PHA staining and HA antibody staining indicating expression and activity in human cells. Nuclei are stained with DAPI, magnification 20×. (B) Transport of EGF fluorescein-bound receptors is rescued by mouse HA-GnT-III expression. OVCAR3 GnT-III siRNA cells were transiently transfected with mouse HA-GnT-III (top panel) or empty vector (bottom panel). Cells were serum-starved for 2 h 1 day after transfection prior to incubation with fluorescein-EGF, as described for Figure 4. (C) OVCAR3 GnT-III siRNA cells were transiently transfected with vector-only or mouse HA-GnT-III prior to plating into 96-well plates. Cells were serum-starved and incubated with vehicle only or EGF 35 ng/mL for 24 h. Cell proliferation was measured using CellTiter Aqueous One (Promega) reagent. Error bars represent the \pm SEM from three separate experiments.

protein fractions suggests high affinity interactions with membrane proteins. We have identified nicastrin (NCSTN) as a glycoprotein enriched by E-PHA specific to serous ovarian cancer. NCSTN is an essential regulator for gamma secretase activity in the Notch pathway.¹⁵ The Notch signaling pathway has been identified by The Cancer Genome Atlas (TCGA) as a pathway significant for the pathophysiology of ovarian cancer.²³ The abundance of glycoproteins known to participate in the Notch signaling pathway that are enriched by E-PHA capture in tumor tissues suggest that this unusual bisecting glycan structure may be important for Notch functions in ovarian carcinoma.

High-grade serous ovarian cancer is the largest fraction of ovarian cancer patients (~80%). The small percentage of membrane glycoproteins that we identified that are unique to this group of cancers following E-PHA capture may offer some insights into why these tumors are so aggressive.

BST2

The BST2 (CD317) is a tetherin glycoprotein that is linked to the membrane via both transmembrane and glycosylphosphatidylinositol (GPI) linkage. This protein is normally expressed in very specialized cells such as paneth cells and in the bone marrow with functions as an intrinsic immunity factor.²⁴ The functions of BST2 in cancer are largely unknown. BST2 expression in breast cancer is associated with metastasis.²⁵ The use of this protein as a therapeutic biomarker for multiple myeloma has been complicated due to expression in nonmalignant bone marrow cells.²⁶ Our discovery of a unique form of glycosylation on this protein in serous ovarian cancer is novel and may allow use of BST2 as a diagnostic or therapeutic target for this solid tumor.

ENG

Endoglin or CD105 is another glycoprotein unique to the serous ovarian carcinoma tumor tissues. Endoglin is a potential marker for mesenchymal stem cell populations.²⁷ A recent study identified endoglin as a potential GPI anchored protein biomarker for breast cancer.⁶ The GPI linkage may explain the increased levels of soluble endoglin in the ascites of ovarian cancer patients.²⁸ Endoglin expression in ovarian cancer is associated with shorter survival.²⁹ A recent study found that endoglin contributes to chemoresistance in ovarian cancer cells.³⁰ Endoglin is typically expressed in endothelial cells at low levels. Therefore, the increased expression levels of endoglin in ovarian cancer coupled to the presence of unique bisecting glycosylation make endoglin a potential therapeutic target for serous ovarian carcinoma.

CDH13

Cadherin-13 or T (truncated) cadherin is an atypical GPI-linked cadherin. CDH13 has been referred to as a tumor suppressor that is dysregulated by epigenetic changes in methylation for many cancers including ovarian cancer.³¹ However, CDH13 has also been demonstrated as a stromal factor that is expressed in the tumor microvascular that can favor tumor growth.³² Also, CDH13 has been shown to associate with cell surface integrins and GRP78 to promote cell survival signaling pathways.³³ Our identification of CDH13 with serous ovarian carcinoma membranes indicates that this protein is expressed in serous ovarian cancer. Future studies will be needed to study the functional impact of CDH13 in ovarian cancer cell survival.

NCSTN

Nicastrin is a component of the γ -secretase (GS) multiprotein enzyme complex responsible for activation of various cell surface membrane proteins including Notch. Nicastrin has been shown

to participate in the regulation of breast cancer stem cell expansion and tumor growth.³⁴ Our identification of nicastrin as a glycoprotein with bisecting glycosylation in serous ovarian carcinoma is novel, and future studies will be needed to determine the role of nicastrin and bisecting glycosylation on ovarian cancer growth and survival.

In conclusion, we present evidence that GnT-III expression is required for the expression of bisecting N-linked glycosylation detected using the lectin E-PHA. Because of the elevated expression levels of GnT-III in ovarian cancer, we have utilized E-PHA for the glycoproteomic analysis of membrane proteins extracted from primary ovarian carcinoma tissues (serous and endometrioid). We identified 100 proteins that were enriched in abundance in tumors demonstrated by an increase in spectral counts by at least 1.5 times following E-PHA capture. Our results suggest new functional roles for bisecting glycosylation in controlling the growth and survival of ovarian cancer. These results may lead to future studies that contribute to the development of new therapeutic interventions for the treatment of ovarian cancer.

■ ASSOCIATED CONTENT

S Supporting Information

Supplementary Table 1. Patient sample information. Supplementary Table 2. Identified peptides for each protein in Table 1 of the manuscript. Supplementary Figure 1. Full MS spectrum. Supplementary Figures 2–4. MSn data analysis. Supplementary Figure 5. Western blot showing EGFR glycosylation and activation in OVCAR3 cells. Supplementary Figure 6. Changes in downstream ERK signaling. This material is available free of charge via the Internet at <http://pubs.acs.org>.

■ AUTHOR INFORMATION

Corresponding Author

*Phone: 501-686-7575. E-mail: kabbott@uams.edu.

Notes

The authors declare no competing financial interest.

■ ACKNOWLEDGMENTS

We thank Rob Bridger and Lance Wells for preliminary technical support. This work was supported by a UO1CA168870 grant from NIH/NCI and a Marsha Rivkin Ovarian Cancer Center Pilot Award.

■ REFERENCES

- (1) Bhaumik, M.; Seldin, M. F.; Stanley, P. Cloning and chromosomal mapping of the mouse Mgat3 gene encoding N-acetylglucosaminyltransferase III. *Gene* **1995**, *164* (2), 295–300.
- (2) Koles, K.; et al. Identification of N-glycosylated proteins from the central nervous system of *Drosophila melanogaster*. *Glycobiology* **2007**, *17* (12), 1388–1403.
- (3) Abbott, K. L.; et al. Targeted glycoproteomic identification of biomarkers for human breast carcinoma. *J. Proteome Res.* **2008**, *7* (4), 1470–1480.
- (4) Tabb, D. L.; Fernando, C. G.; Chambers, M. C. MyriMatch: highly accurate tandem mass spectral peptide identification by multivariate hypergeometric analysis. *J. Proteome Res.* **2007**, *6* (2), 654–661.
- (5) Ma, Z. Q.; et al. IDPicker 2.0: Improved protein assembly with high discrimination peptide identification filtering. *J. Proteome Res.* **2009**, *8* (8), 3872–3881.
- (6) Zhao, P.; et al. Proteomic identification of glycosylphosphatidylinositol anchor-dependent membrane proteins elevated in breast carcinoma. *J. Biol. Chem.* **2012**, *287* (30), 25230–25240.

- (7) Abbott, K. L.; et al. Focused glycomic analysis of the N-linked glycan biosynthetic pathway in ovarian cancer. *Proteomics* **2008**, *8* (16), 3210–3220.
- (8) Abbott, K. L.; et al. Identification of candidate biomarkers with cancer-specific glycosylation in the tissue and serum of endometrioid ovarian cancer patients by glycoproteomic analysis. *Proteomics* **2010**, *10* (3), 470–481.
- (9) Anugraham, M. Specific glycosylation of membrane proteins in epithelial ovarian cancer cell lines: glycan structures reflect gene expression and DNA methylation status. *Mol. Cell. Proteomics* **2014**, *13*, 2213–2232.
- (10) Uhlen, M.; et al. Towards a knowledge-based Human Protein Atlas. *Nat. Biotechnol.* **2010**, *28* (12), 1248–1250.
- (11) Wang, M. M. Notch signaling and Notch signaling modifiers. *Int. J. Biochem. Cell Biol.* **2011**, *43* (11), 1550–1562.
- (12) Wesley, C. S. Notch and wingless regulate expression of cuticle patterning genes. *Mol. Cell. Biol.* **1999**, *19* (8), 5743–5758.
- (13) Nehring, L. C.; et al. The extracellular matrix protein MAGP-2 interacts with Jagged1 and induces its shedding from the cell surface. *J. Biol. Chem.* **2005**, *280* (21), 20349–20355.
- (14) VanDussen, K. L.; et al. Notch signaling modulates proliferation and differentiation of intestinal crypt base columnar stem cells. *Development* **2012**, *139* (3), 488–497.
- (15) Li, T.; et al. Nicastin is required for assembly of presenilin/gamma-secretase complexes to mediate Notch signaling and for processing and trafficking of beta-amyloid precursor protein in mammals. *J. Neurosci.* **2003**, *23* (8), 3272–3277.
- (16) Horiguchi, M.; Ota, M.; Rifkin, D. B. Matrix control of transforming growth factor-beta function. *J. Biochem.* **2012**, *152* (4), 321–329.
- (17) Meurer, S. K.; et al. Overexpression of endoglin modulates TGF-beta1-signalling pathways in a novel immortalized mouse hepatic stellate cell line. *PLoS One* **2013**, *8* (2), e56116.
- (18) Barbolina, M. V.; et al. Matrix rigidity activates Wnt signaling through down-regulation of Dickkopf-1 protein. *J. Biol. Chem.* **2013**, *288* (1), 141–151.
- (19) Takahashi, T.; et al. alpha1,6fucosyltransferase is highly and specifically expressed in human ovarian serous adenocarcinomas. *Int. J. Cancer* **2000**, *88* (6), 914–919.
- (20) Song, Y.; et al. The bisecting GlcNAc on N-glycans inhibits growth factor signaling and retards mammary tumor progression. *Cancer Res.* **2010**, *70* (8), 3361–3371.
- (21) North, S. J.; et al. Glycomics profiling of Chinese hamster ovary cell glycosylation mutants reveals N-glycans of a novel size and complexity. *J. Biol. Chem.* **2010**, *285* (8), 5759–5775.
- (22) Yang, X.; et al. Structures and biosynthesis of the N- and O-glycans of recombinant human oviduct-specific glycoprotein expressed in human embryonic kidney cells. *Carbohydr. Res.* **2012**, *358*, 47–55.
- (23) Cancer Genome Atlas Research, N.. Integrated genomic analyses of ovarian carcinoma. *Nature* **2011**, *474* (7353), 609–615.
- (24) Blasius, A. L.; et al. Bone marrow stromal cell antigen 2 is a specific marker of type I IFN-producing cells in the naive mouse, but a promiscuous cell surface antigen following IFN stimulation. *J. Immunol.* **2006**, *177* (5), 3260–3265.
- (25) Cai, D.; et al. Up-regulation of bone marrow stromal protein 2 (BST2) in breast cancer with bone metastasis. *BMC Cancer* **2009**, *9*, 102.
- (26) Tai, Y. T.; et al. Potent in vitro and in vivo activity of an Fc-engineered humanized anti-HM1.24 antibody against multiple myeloma via augmented effector function. *Blood* **2012**, *119* (9), 2074–2082.
- (27) Jeong, J. A.; et al. Membrane proteomic analysis of human mesenchymal stromal cells during adipogenesis. *Proteomics* **2007**, *7* (22), 4181–4191.
- (28) Bock, A. J.; et al. Endoglin (CD105) expression in ovarian serous carcinoma effusions is related to chemotherapy status. *Tumour Biol.* **2011**, *32* (3), 589–596.
- (29) Henriksen, R.; et al. Expression and prognostic significance of TGF-beta isotypes, latent TGF-beta 1 binding protein, TGF-beta type I and type II receptors, and endoglin in normal ovary and ovarian neoplasms. *Lab. Invest.* **1995**, *73* (2), 213–220.
- (30) Ziebarth, A. J.; et al. Endoglin (CD105) contributes to platinum resistance and is a target for tumor-specific therapy in epithelial ovarian cancer. *Clin. Cancer Res.* **2013**, *19* (1), 170–182.
- (31) Chmelarova, M.; et al. Methylation analysis of tumour suppressor genes in ovarian cancer using MS-MLPA. *Folia Biol. (Prague, Czech Repub.)* **2012**, *58* (6), 246–250.
- (32) Ghosh, S.; et al. Use of multicellular tumor spheroids to dissect endothelial cell-tumor cell interactions: a role for T-cadherin in tumor angiogenesis. *FEBS Lett.* **2007**, *581* (23), 4523–4528.
- (33) Philippova, M.; et al. Identification of proteins associating with glycosylphosphatidylinositol-anchored T-cadherin on the surface of vascular endothelial cells: role for Grp78/BiP in T-cadherin-dependent cell survival. *Mol. Cell. Biol.* **2008**, *28* (12), 4004–4017.
- (34) Lombardo, Y.; et al. Nicastin regulates breast cancer stem cell properties and tumor growth in vitro and in vivo. *Proc. Natl. Acad. Sci. U. S. A.* **2012**, *109* (41), 16558–16563.